Relativistically corrected nuclear magnetic resonance chemical shifts calculated with the normalized elimination of the small component using an effective potential-NMR chemical shifts of molybdenum and tungsten

Michael Filatov and Dieter Cremer
Department of Theoretical Chemistry, Göteborg University, Reutersgatan 2, S-413 20 Göteborg, Sweden

(Received 12 March 2003; accepted 15 April 2003)

A new method for relativistically corrected nuclear magnetic resonance (NMR) chemical shifts is developed by combining the individual gauge for the localized orbital approach for density functional theory with the normalized elimination of a small component using an effective potential. The new method is used for the calculation of the NMR chemical shifts of ^{95}Mo and ^{183}W in various molybdenum and tungsten compounds. It is shown that quasirelativistic corrections lead to an average improvement of calculated NMR chemical shift values by 300 and 120 ppm in the case of ^{95}Mo and ^{183}W, respectively, which is mainly due to improvements in the paramagnetic contributions. The relationship between electronic structure of a molecule and the relativistic paramagnetic corrections is discussed. Relativistic effects for the diamagnetic part of the magnetic shielding caused by a relativistic contraction of the s,p orbitals in the core region concern only the shielding values, however, have little consequence for the shift values because of the large independence from electronic structure and a cancellation of these effects in the shift values. It is shown that the relativistic corrections can be improved by level shift operators and a B3LYP hybrid functional, for which Hartree–Fock exchange is reduced to 15%. © *2003 American Institute of Physics.* [DOI: 10.1063/1.1580091]

I. INTRODUCTION

The calculation of magnetic shieldings and nuclear magnetic resonance (NMR) chemical shifts has substantially broadened the applicability of quantum chemical methods for practical purposes and is now an important asset of most quantum chemical investigations.[1–4] Gauge-invariant or at least approximately gauge-invariant methods at the electron correlation corrected *ab initio* levels have led to a wealth of reliable NMR chemical shift data concerning in particular first and second row nuclei.[4–13] Bouman and Hansen[5] were the first to extend their localized orbital/local origin (LORG) approach[14] with the help of the second order polarization propagator (SOPPA),[15] so that electron correlation effects were included up to second order. Independently, a SOPPA method for calculating NMR chemical shifts was also published by Oddershede and Sauer.[6] Gauss and co-workers[4,7–11] developed the gauge-including atomic orbitals (GIAO) method[16] previously applied only at the Hartree–Fock (HF) level[17,18] at the nth order ($n=2,3,4$) many body perturbation theory with the Møller–Plesset perturbation (MPn) and at coupled cluster theory level yielding in this way GIAO-MP2,[7] GIAO-MP3,[8] GIAO-MP4,[8] GIAO-CCSD,[9] and GIAO-CCSD(T).[10] Later, GIAO was extended to the domain of density functional theory (DFT).[19,20] GIAO was also extended to multiconfigurational self-consistent field (MCSCF) theory (GIAO-MCSCF) (Ref. 12) as was the individual gauge for localized orbitals (IGLO) method of Schindler and Kutzelnigg[21,22] that led to IGLO-MCSCF.[13]

The correlation corrected GIAO, LORG, and IGLO methods provide accurate shielding and NMR chemical shift data, which can clarify or complement contradictory, unusual or incomplete NMR experiments so that the calculated NMR chemical shifts represent an important tool for the experimentalist. The IGLO method has been successful in the realm of Hartree–Fock calculations while its extension to MCSCF was used less because of cost reasons. Instead, its density functional theory counterpart IGLO-DFT (Refs. 23, 24) has been used extensively for larger molecules,[25–27] for which correlated GIAO methods, even when integral-direct methods are applied,[28] are too costly to be carried out. IGLO-DFT is a method that has to include empirical corrections[23–25] to compensate a basic failure of DFT, namely, to exaggerate paramagnetic contributions to magnetic shielding constants because the occupied orbitals of a molecule are generally predicted to be too high in energy at the DFT level of theory.[29] Nevertheless, IGLO-DFT can be considered as the most economic approach for obtaining reasonable NMR chemical shifts for large molecules. The reliability of IGLO-DFT is given by the fact that the gradient corrected exchange functionals nowadays used include both dynamic and nondynamic electron correlation effects[30,31] thus leading to reasonable shift values.

Relativity strongly modifies the electron distribution in the vicinity of the nucleus and consequently all properties, which depend on the electronic density in regions close to the nucleus. The inclusion of relativistic effects is mandatory in the calculation of NMR shielding of heavy nuclei.[20] The scalar relativistic (spin-independent) effects are particularly important for heavy transition metals, whereas the spin–orbit effects result in a modest modification of shielding comparable with environmental effects.[20] Thus, the scalar-

 © 2003 American Institute of Physics

Downloaded 25 Jan 2005 to 129.16.100.69. Redistribution subject to AIP license or copyright, see http://jcp.aip.org/jcp/copyright.jsp

relativistic (SR) approximation is in many cases sufficient to study NMR shielding of heavy transition metal nuclei in complexes.[20]

We have recently developed a new quasirelativistic method within the normalized elimination of the small component (NESC) approximation.[32–34] The purpose of this development is to have a method available, which is variationally stable, and can be easily implemented in any nonrelativistic quantum-chemical program, which leads to reliable relativistic corrections, and which requires low computational cost so that its application to large molecules is feasible. These requirements are fulfilled by the NESC approach[35] using an effective potential (NESC-EP method[32]), which if carried out for density functional theory [NESC-EP-DFT (Refs. 33, 34)] represents one of the easiest and most economic quasirelativistic approaches.

Apart from its accuracy, an important feature of NESC-EP is its simplicity both in the sense of implementation and in the sense of computational cost. The matrix elements of the NESC-EP-DFT Hamiltonian do not involve any unusual molecular integrals often appearing in relativistic calculations; they can be evaluated analytically using the existing nonrelativistic quantum-chemical software. Since all modifications concern the one-electron Hamiltonian only, the results of the relativistic calculation can be obtained at essentially the cost of a nonrelativistic calculation.

As the NESC-EP-DFT method treats all electrons explicitly, it can be used for the calculation of magnetic shielding tensors of heavy elements in large molecular systems. In this work we develop the theory of a NESC-EP-based individual gauge for the localized orbital approach for density functional theory (IGLO-DFT) to obtain a reliable and easily applicable method for the calculation of relativistically corrected NMR chemical shifts. The new method, IGLO-NESC-EP-DFT, will be applied to obtain NMR chemical shifts for molybdenum and tungsten compounds. In this connection we will demonstrate how by the use of the appropriate exchange-correlation functional and level shift operators, reasonable shift values are obtained for these heavy nuclei.

In Sec. II, the theory of IGLO-NESC-EP-DFT will be described and in Sec. III the implementation of the new method as well as the computational ingredients needed to apply it. Calculated NMR chemical shifts for the Mo and W compounds investigated in this work are listed and discussed in Sec. IV. Section V gives conclusions and an outlook on future developments concerning IGLO-NESC-EP-DFT is given.

II. THEORY OF IGLO-NESC-EP-DFT

In the following, we shortly describe the nonrelativistic IGLO-DFT formalism (Sec. II A), before we discuss the NESC-EP method (Sec. II B) and the new IGLO-NESC-EP-DFT approach for calculating NMR chemical shifts of heavy elements. In Sec. II C, the implementation of the new method and the computational procedures to use it in the case of molybdenum and tungsten compounds is described.

A. The nonrelativistic IGLO formalism

For a closed-shell molecule, the DFT-IGLO expression for the nuclear magnetic shielding tensor is[24]

$$(\sigma^A)_{\alpha\beta}=\frac{\partial^2 E(\mu^A,\mathbf{B})}{\partial\mu^A_\alpha\partial\mathbf{B}_\beta}=2\sum_i^{\text{occ}}\langle\phi_i^{(0)}|\hat{h}^{11}_{i,\alpha\beta}|\phi_i^{(0)}\rangle-4\sum_i^{\text{occ}}\langle\phi_i^{(0)}|\hat{h}^{01}_{\alpha}|\phi^{(\mathbf{B})}_{i,\beta}\rangle, \quad (1)$$

where $\mathbf{B}$ denotes the external magnetic field, $\phi_i^{(0)}$ and $\phi_i^{(\mathbf{B})}$ are doubly occupied zeroth order and first order Kohn–Sham (KS) orbitals[36] localized according to the criterion of Foster and Boys,[37] the index A refers to the nucleus in question, and the α and β subscripts denote the Cartesian coordinates x, y, or z. The one-electron magnetic operators are defined by

$$\hat{h}^{11}_{i,\alpha\beta}=\frac{\partial^2\hat{H}^{11}_i}{\partial\mu^A_\alpha\partial\mathbf{B}_\beta}=\frac{e^2}{2mc^2}\frac{\delta_{\alpha\beta}(\mathbf{r}-\mathbf{R}_i)\cdot(\mathbf{r}-\mathbf{R}_A)-(\mathbf{r}-\mathbf{R}_i)_\alpha(\mathbf{r}-\mathbf{R}_A)_\beta}{|\mathbf{r}-\mathbf{R}_A|^3} \quad (2)$$

and

$$\hat{h}^{01}_{\alpha}=\frac{1}{i}\frac{\partial\hat{H}^{01}}{\partial\mu^A_\alpha}=-\frac{e}{mc}\frac{(\mathbf{r}-\mathbf{R}_A)\times\nabla}{|\mathbf{r}-\mathbf{R}_A|^3} \quad (3)$$

(e, electron charge; m, mass of an electron; c, speed of light), where the superscripts 0 and 1 define the order of the operator in the magnetic field $\mathbf{B}$ (first superscript) and in the magnetic moment μ^A of the nucleus A (second superscript). The position vector $\mathbf{R}_A$ gives the location of nucleus A and $\mathbf{r}$ is the position of an electron in localized orbital ϕ_i. The expressions for the operators $\hat{H}^{11}$ and $\hat{H}^{01}$ can be found in many publications and are not reproduced here.

The first-order occupied Kohn–Sham orbitals $\phi_i^{(\mathbf{B})}$ are expanded in terms of the zero-order (unperturbed) KS orbitals according to

$$\phi_i^{(\mathbf{B})}=\sum_j^{\text{occ}}\phi_j^{(0)}\mathbf{O}_{ji}+\sum_a^{\text{virt}}\phi_a^{(0)}\mathbf{O}_{ai}. \quad (4)$$

The occupied–occupied part of the matrix $\mathbf{O}$ represents the projection of the first-order KS orbitals onto the zero-order KS orbitals and is not defined uniquely. Within the IGLO approach it is chosen as

$$\mathbf{O}_{ji}=-\frac{e}{2mc}\langle\phi_j^{(0)}|\mathbf{\Lambda}_j^{(\mathbf{B})}-\mathbf{\Lambda}_i^{(\mathbf{B})}|\phi_i^{(0)}\rangle, \quad (5)$$

where

$$\mathbf{\Lambda}_i^{(\mathbf{B})}=\tfrac{1}{2}(\mathbf{R}_i\times\mathbf{r}), \quad (6)$$

which is compatible with the orthonormality restriction of the KS orbitals. The occupied-virtual part of the matrix $\mathbf{O}$ is given by

$$\mathbf{O}_{ai}=\sum_k^{\text{occ}}\left(\frac{\sum_j^{\text{occ}}\mathbf{Y}_{aj}c_{kj}}{\epsilon_k-\epsilon_a}\right)c_{ki}, \quad (7)$$

Downloaded 25 Jan 2005 to 129.16.100.69. Redistribution subject to AIP license or copyright, see http://jcp.aip.org/jcp/copyright.jsp

where

$$\mathbf{Y}_{ai}=\langle\phi_a^{(0)}|\hat{h}_i^{10}|\phi_i^{(0)}\rangle-\frac{e}{c}\sum_j^{\text{occ}}\langle\phi_a^{(0)}|\mathbf{\Lambda}_i^{(\mathbf{B})}-\mathbf{\Lambda}_j^{(\mathbf{B})}|\phi_j^{(0)}\rangle \times\langle\phi_j^{(0)}|\hat{f}^{(0)}|\phi_i^{(0)}\rangle. \quad (8)$$

In Eq. (8), the zero-order virtual orbitals $\phi_a^{(0)}$ are the usual canonical orbitals, the one-electron operator $\hat{h}_i^{10}$ is defined by

$$\hat{h}_i^{10}=\frac{1}{i}\frac{\partial\hat{H}_i^{10}}{\partial\mathbf{B}}=-\frac{e}{2mc}(\mathbf{r}-\mathbf{R}_i)\times\nabla \quad (9)$$

and the unperturbed KS one-electron operator is given by

$$\hat{f}^{(0)}=\frac{\mathbf{p}^2}{2m}+\sum_C -\frac{Z_C}{|\mathbf{r}-\mathbf{R}_C|}+\int\frac{\rho(\mathbf{r}')}{|\mathbf{r}-\mathbf{r}'|}d\mathbf{r}'+V_{\text{xc}}(\mathbf{r}), \quad (10)$$

where $\mathbf{p}$ is the linear momentum operator, Z_C is the nuclear charge, $\rho(\mathbf{r})$ denotes the electron density, and $V_{\text{xc}}(\mathbf{r})$ denotes the usual exchange-correlation potential. With the use of approximate pure density functionals, the dependence of V_{xc} on the first-order orbitals $\phi_i^{(\mathbf{B})}$ vanishes and the uncoupled DFT-IGLO (UC-DFT-IGLO) approach results. The dependence on the first-order orbitals can be introduced either via the use of the level shift operators, such as the Loc.1 and Loc.2 operators suggested by Malkin *et al.*[23] [the level shift, which corrects for an underestimation of the energy gap between the frontier orbitals in DFT, is constructed via the first-order (perturbed) density], or via the use of hybrid density functionals, such as B3LYP,[38] that mix in a fraction of the Hartree–Fock exchange energy.[21,22] In both cases, the solution of Eq. (7) depends on the first-order orbitals $\phi_i^{(\mathbf{B})}$ and the equation is solved iteratively.

B. The relativistic NESC-EP method and IGLO-NESC-EP-DFT

Expanding the unperturbed one-electron orbitals $\phi_i^{(0)}$ in terms of (nonorthogonal) basis set functions χ according to Eq. (11),

$$\phi_i^{(0)}=|\chi\rangle\mathbf{C}_i \quad (11)$$

($|\chi\rangle$, row-vector of basis functions; $\mathbf{C}_i$, column-vector of expansion coefficients) the scalar-relativistic NESC-EP equations within the KS formalism[33] are given in matrix form by Eq. (12),

$$((\mathbf{S}^{1/2})^\dagger(\mathbf{U}^{-1/2})^\dagger\mathbf{H}(\mathbf{U}^{-1/2})(\mathbf{S}^{1/2})+\mathbf{J}+\mathbf{V}_{\text{xc}})\mathbf{C}_i=\mathbf{S}\mathbf{C}_i\boldsymbol{\epsilon}_i, \quad (12)$$

where $\mathbf{J}$ and $\mathbf{V}_{\text{xc}}$ are the matrices of the classical Coulomb repulsion operator and of the Kohn–Sham potential, the renormalization matrix $\mathbf{U}$ is given in Eq. (13),

$$\mathbf{U}=\mathbf{S}+\frac{1}{2mc^2}\mathbf{T} \quad (13)$$

and the one-electron Hamiltonian matrix $\mathbf{H}$ is given in Eq. (14),

$$\mathbf{H}=\mathbf{T}+\mathbf{V}+\mathbf{W}. \quad (14)$$

In Eqs. (13) and (14), $\mathbf{S}$ is the matrix of the overlap integrals, $\mathbf{T}$ and $\mathbf{V}$ are the matrices of the kinetic energy and electron-nuclear attraction operators, and $\mathbf{W}$ denotes the matrix of the operator $(1/4m^2c^2)\mathbf{p}V'_{Ne}\cdot\mathbf{p}$, where the effective potential V'_{Ne} is given in Eq. (15),

$$V'_{Ne}(\mathbf{r})=\sum_A -\frac{Z_A}{|\mathbf{r}-\mathbf{R}_A|}\text{erf}(|\mathbf{r}-\mathbf{R}_A|/r_0(Z_A)). \quad (15)$$

In Eq. (15), $r_0(Z_A)$ is a cut-off radius specific for the nucleus A and $\mathbf{R}_A$ is the position of the nucleus A. The dependence of $r_0(Z_n)$ on the nuclear charge is given in Eq. (16),[32,33]

$$r_0(Z)=(a_0+a_1Z^{-1}+a_2Z^{-2})\frac{Z}{mc^2} \quad (16)$$

with the coefficients $a_0=-0.263\,188$, $a_1=106.016\,974$, $a_2=138.985\,999$ being based on a fit of the $1s_{1/2}$ eigenvalues of the Dirac equation for H-like atomic ions.

In the presence of a magnetic field with the vector potential $\mathbf{A}$, the linear momentum operator couples to the field via Eq. (17),

$$\pi=\mathbf{p}+\frac{e}{c}\mathbf{A}. \quad (17)$$

Thus, the expressions for the matrix elements of the renormalization matrix $\mathbf{U}$ and the one-electron Hamiltonian $\mathbf{H}$ modify to

$$\begin{aligned}\mathbf{U}_{\mu\nu}^{(\mathbf{A})}&=\langle\chi_\mu|1+\frac{\pi^2}{4m^2c^2}|\chi_\nu\rangle\\&=\langle\chi_\mu|1+\frac{\mathbf{p}^2}{4m^2c^2}|\chi_\nu\rangle+\frac{e}{4m^2c^3}\langle\chi_\mu|\mathbf{p}\cdot\mathbf{A}+\mathbf{A}\cdot\mathbf{p}|\chi_\nu\rangle\\&\quad+\frac{e^2}{4m^2c^4}\langle\chi_\mu|\mathbf{A}^2|\chi_\nu\rangle=\mathbf{U}_{\mu\nu}^{(0)}+O(c^{-3}),\end{aligned} \quad (18)$$

$$\begin{aligned}\mathbf{H}_{\mu\nu}^{(\mathbf{A})}&=\langle\chi_\mu|\frac{\pi^2}{2m}+V_{Ne}+\frac{1}{4m^2c^2}\pi V'_{Ne}\cdot\pi|\chi_\nu\rangle\\&=\langle\chi_\mu|\frac{\mathbf{p}^2}{2m}+V_{Ne}+\frac{1}{4m^2c^2}\mathbf{p}V'_{Ne}\cdot\mathbf{p}|\chi_\nu\rangle\\&\quad+\frac{e}{2mc}\langle\chi_\mu|\mathbf{p}\cdot\mathbf{A}+\mathbf{A}\cdot\mathbf{p}|\chi_\nu\rangle+\frac{e^2}{2mc^2}\langle\chi_\mu|\mathbf{A}^2|\chi_\nu\rangle\\&\quad+\frac{e}{4m^2c^3}\langle\chi_\mu|\mathbf{p}V'_{Ne}\cdot\mathbf{A}+\mathbf{A}V'_{Ne}\cdot\mathbf{p}|\chi_\nu\rangle\\&\quad+\frac{e^2}{4m^2c^4}\langle\chi_\mu|V'_{Ne}\mathbf{A}^2|\chi_\nu\rangle\\&=\mathbf{H}_{\mu\nu}^{(0)}+\frac{e}{2mc}\langle\chi_\mu|\mathbf{p}\cdot\mathbf{A}+\mathbf{A}\cdot\mathbf{p}|\chi_\nu\rangle\\&\quad+\frac{e^2}{2mc^2}\langle\chi_\mu|\mathbf{A}^2|\chi_\nu\rangle+O(c^{-3}).\end{aligned} \quad (19)$$

Downloaded 25 Jan 2005 to 129.16.100.69. Redistribution subject to AIP license or copyright, see http://jcp.aip.org/jcp/copyright.jsp

In calculations of the NMR shielding tensor, the high order relativistic corrections (c^{-3} and c^{-4}) to the magnetic terms in Eqs. (18) and (19) are neglected. Truncating **U** and **H** at the second order in c^{-1} recovers the same magnetic terms that appear in the scalar-relativistic theory based on the Pauli Hamiltonian.[22] This can be verified by substituting the last lines of Eqs. (18) and (19) into Eq. (12) and expanding $\mathbf{U}_{\mu\nu}^{(0)}$ in powers of c^{-2}. The most significant contributions beyond this approximation are the spin–orbit contributions, which are not taken into account in the present work. The terms neglected in Eqs. (18) and (19) are smaller in magnitude than the spin–orbit terms. Thus, neglecting them is consistent with other approximations made in the present work. Substituting Eq. (20),

$$\mathbf{A}=\frac{1}{2}\mathbf{B}\times(\mathbf{r}-\mathbf{R}_i)+\frac{\mu^A\times(\mathbf{r}-\mathbf{R}_A)}{|\mathbf{r}-\mathbf{R}_A|^3} \tag{20}$$

for the vector potential **A** of a homogeneous magnetic field **B** (with the gauge origin at $\mathbf{R}_i$) and a magnetic nucleus with permanent magnetic moment μ (at a location $\mathbf{R}_A$) into the last lines of Eqs. (18) and (19) and differentiating with respect to the magnetic field and the nuclear magnetic moment one arrives at the following expressions for the matrix elements of the $\hat{h}^{11}$, $\hat{h}^{10}$, and $\hat{h}^{01}$ operators in the IGLO-NESC-EP approach;

$$\begin{aligned}\langle\chi_\mu|^{\text{NESC-EP}}\hat{h}^{11}_{i,\alpha\beta}|\chi_\nu\rangle &= \frac{e^2}{2mc^2}\sum_{\rho,\tau}\mathbf{X}_{\rho\mu}\\ &\times\langle\chi_\rho|\frac{\delta_{\alpha\beta}(\mathbf{r}-\mathbf{R}_i)\cdot(\mathbf{r}-\mathbf{R}_A)-(\mathbf{r}-\mathbf{R}_i)_\alpha(\mathbf{r}-\mathbf{R}_A)_\beta}{|\mathbf{r}-\mathbf{R}_A|^3}|\chi_\tau\rangle\\ &\times\mathbf{X}_{\tau\nu},\end{aligned} \tag{21}$$

$$\langle\chi_\mu|^{\text{NESC-EP}}\hat{h}^{01}_{\alpha}|\chi_\nu\rangle = -\frac{e}{mc}\sum_{\rho,\tau}\mathbf{X}_{\rho\mu}\langle\chi_\rho|\frac{(\mathbf{r}-\mathbf{R}_A)\times\nabla}{|\mathbf{r}-\mathbf{R}_A|^3}|\chi_\nu\rangle\mathbf{X}_{\tau\nu}, \tag{22}$$

$$\langle\chi_\mu|^{\text{NESC-EP}}\hat{h}^{10}_{i}|\chi_\nu\rangle = -\frac{e}{2mc}\sum_{\rho,\tau}\mathbf{X}_{\rho\mu}\langle\chi_\rho|(\mathbf{r}-\mathbf{R}_i)\times\nabla|\chi_\tau\rangle\mathbf{X}_{\tau\nu}, \tag{23}$$

where **X** stands for

$$\mathbf{X}=\mathbf{U}^{-1/2}\mathbf{S}^{1/2}. \tag{24}$$

Thus, within the present approach the usual nonrelativistic magnetic integrals used in the IGLO method are renormalized using the quasirelativistic metric of the NESC-EP method.

C. Implementation and computational procedures

The IGLO-NESC-EP-DFT method was programmed and incorporated into the COLOGNE 2003 suite of quantum-chemical programs.[39] The one-electron integrals and integral derivatives necessary to carry out a NESC-EP calculation were implemented according to Refs. 32–34. The IGLO-NESC-EP-DFT program is based on the nonrelativistic IGLO-DFTO program developed by Olsson and Cremer.[24] The relativistic corrections require a renormalization of the standard magnetic one-electron integrals as described in the preceding section. Because only the one-electron molecular integrals are modified in the present approach, the computational cost of a IGLO-NESC-EP-DFT quasirelativistic calculation is essentially the same as the task of a nonrelativistic IGLO-DFT calculation.

The IGLO-NESC-EP-DFT method was tested for ^{13}C-, ^{15}N-, and ^{17}O-shieldings σ and the corresponding NMR chemical shifts δ of some small molecules (see Table I) using the MP2 molecular geometries of Gauss,[7] the B3LYP functional,[38,40,41] the $(11s,7p,2d/5s,1p)[7s,6p,2d/4s,2p]$ basis set,[22] and CH_4, NH_3, and H_2O molecules as appropriate references for the shift values. For the molecules of Table I, we expect small relativistic corrections generally smaller than 1 ppm because larger scalar relativistic effects occur only for $Z>36$. This expectation is confirmed by the calculated IGLO-NESC-EP-B3LYP data, which are compared in Table I with the corresponding IGLO-B3LYP data by giving the relativistic correction in parentheses. All relativistic corrections for the shielding are negative and, in view of the very small corrections for the reference molecules, all chemical shift corrections become positive. The (absolute) magnitude of the relativistic effects for the ^{17}O-shieldings is somewhat larger (0.5–3.7 ppm) while those for ^{13}C- and ^{15}N-shieldings are all smaller than 1 ppm. A shielding of the nucleus because of a relativistic contraction of the core orbitals would lead to somewhat more negative shift values (shifts to higher field). Hence, the small relativistic corrections calculated result from a dominance of the relativistic corrections to the paramagnetic contributions. We find that these are -0.1 to -3.9 ppm while the relativistic corrections of the diamagnetic contributions are 0.1–0.3 ppm. Within the IGLO approach, the definition of diamagnetic and paramagnetic contribution is method immanent and done in a way to minimize the former.[21,22] Hence, diamagnetic and paramagnetic IGLO contributions have no relationship to measurable quantities. Nevertheless, we have found it useful in this work to use these quantities to analyze the relativistic corrections calculated, for example by setting them into relationship to the electronic structure of a molecule.

For the calculation of molybdenum and tungsten compounds investigated in this work, basis sets of Gropen[42] were modified in the following way. In the case of molybdenum, a $[15s7p8d]$ basis set was constructed from Gropen's $(17s12p8d)$ basis set of primitive Gaussian-type functions (GTF).[42] The most tight *s*-type primitive remains uncontracted along with thirteen diffuse *s*-type primitives. The remaining three *s*-type GTFs are contracted using the coefficients for the $1s$ atomic orbital formed from the original uncontracted set. The five most diffuse *p*-type GTF also remain uncontracted. The four most tight *p*-type primitives are contracted using the coefficients of the $2p$ atomic orbital of the original set and the next three *p*-type primitives are contracted using the coefficients of the $3p$ atomic orbital of the

Downloaded 25 Jan 2005 to 129.16.100.69. Redistribution subject to AIP license or copyright, see http://jcp.aip.org/jcp/copyright.jsp

TABLE I. Magnetic shieldings and NMR chemical shifts calculated with IGLO-NESC-EP-B3LYP for some first row molecules.[a]

		IGLO		Loc.1		Loc.2		Expt.
Molecule	Nucleus	σ	δ	σ	δ	σ	δ	δ
CH_4	C	189.7 (0)	0	191.1 (0)	0	191.5 (0)	0	0
NH_3	N	258.5 (0)	0	260.0 (−0.1)	0	260.6 (0)	0	0
H_2O	O	320.5 (−0.1)	0	323.0 (−0.1)	0	323.8 (−0.1)	0	0
CO	C	−22.3 (−0.2)	212.0	−6.9 (−0.2)	198.0	−2.3 (−0.1)	193.8	194.1
	O	−89.0 (−1.1)	409.5	−65.6 (−0.9)	388.6	−58.6 (−0.9)	382.4	386.3
CO_2	C	46.8 (−0.2)	142.9	48.6 (−0.2)	142.5	49.2 (−0.2)	142.3	136.3
	O	208.0 (−0.5)	112.5	212.0 (−0.5)	111.0	213.3 (−0.5)	110.5	100.6
CF_4	C	42.9 (−0.3)	146.8	44.2 (−0.3)	146.9	44.6 (−0.3)	146.9	130.6
CH_2O	C	−27.3 (−0.2)	217.0	−18.5 (−0.1)	209.6	−15.8 (−0.2)	207.3	···
	O	−474.1 (−1.6)	794.6	−425.7 (−1.5)	748.7	−410.9 (−1.5)	734.7	···
HCN	C	67.4 (−0.1)	122.3	72.2 (0)	118.9	73.7 (0.1)	117.8	113.0
	N	−54.2 (−0.3)	312.7	−40.9 (−0.3)	300.9	−36.7 (−0.3)	297.3	284.9
N_2	N	−105.0 (−0.6)	363.5	−87.5 (−0.5)	347.5	−82.1 (−0.5)	342.7	326.1
N_2O	N1	−20.0 (−0.5)	278.5	−13.8 (−0.5)	273.8	−11.8 (−0.5)	272.4	253.2
(N2N1O)	N2	75.5 (−0.5)	183.0	83.8 (−0.5)	176.2	86.4 (−0.5)	174.2	165.0
	O	153.4 (−1.3)	167.1	161.7 (−1.3)	161.3	164.4 (−1.3)	159.4	143.4
OF_2	O	−630.1 (−3.7)	950.6	−567.4 (−3.4)	890.4	−548.6 (−3.3)	872.4	817.1

[a]Magnetic shieldings σ and NMR chemical shifts δ in ppm. MP2/tzp geometries from Ref. 7(b) are used. Relativistic effects given as σ (IGLO-NESC-EP-B3LYP)-σ(IGLO-B3LYP) in parentheses. The level shift operators Loc.1 and Loc.2 are defined in Refs. 23 and 24. Experimental values are taken from a compilation given in Ref. 7(b).

original set. All *d*-type GTF remain uncontracted. The $[15s7p8d]$ basis set is extended to a $[16s10p9d]$ set by amending the former by one *s*-type, three *p*-type, and one *d*-type diffuse GTF in a well-tempered sequence using the exponent ratio of 2.5.

For tungsten, a $[16s12p8d4f]$ basis set constructed from the $(19s14p10d5f)$ basis set of Gropen[42] is used. The three most tight *s*-type primitives remain uncontracted along with eight diffuse *s*-type primitives. The remaining seven *s*-type primitives are block-contracted in a sequence (3/2/2/2) using the contraction coefficients from $1s$, $2s$, $3s$, and $4s$ atomic orbital formed from the $(19s14p10d5f)$ set. The last two contracted *s*-functions in this sequence share one common primitive. The five most diffuse *p*-type primitives remain uncontracted while the other nine *p*-type primitives are block-contracted in a sequence (3/3/2/2) using the coefficients from the $2p$, $3p$, $4p$, and $5p$ atomic orbital formed with the original set. The second and the third contracted *p*-function share one common *p*-type GTF. The most diffuse *d*-type primitive is dropped due to orthogonality problems. The next two diffuse *d*-type GTF remain uncontracted. The remaining seven *d*-type primitives are block-contracted in the sequence (4/2/2) using the contraction coefficients from the $3d(4/2)$ and the $4d$ orbital of the original set. The last two contracted *d*-type basis functions share one common primitive GTF. The two most tight *f*-type primitives are contracted. The $[15s9p7d3f]$ basis set obtained is amended by one *s*-type, three *p*-, one *d*-type, and one *f*-type primitives (according to a well-tempered sequence with ratio 2.5) thus leading to the final $[16s12p8d4f]$ basis set.

For elements O and F, a $(9s,5p,1d)[6s,4p,1d]$ and for S and Cl a $(11s6p2d)[7s8p2d]$ basis set is used developed for the calculation of magnetic properties.[22] The $[9s8p4d]$ basis set on Se is constructed from Dunning's cc-pVDZ basis set[43] by recontracting it in the following way: The five first *s*-type primitives are contracted using the contraction coefficients from the $1s$ atomic orbital in the original set. The next two *s*-type primitives are contracted with the coefficients from the second $2s$ atomic orbital formed from the original basis set. All other *s*-type GTFs remain uncontracted. The three first *p*-type primitives are contracted using the coefficients of the $2p$ atomic orbital of the original set. The next two *p*-type primitives are contracted with the coefficients from the $3p$ atomic orbital while all other *p*-type primitives remain uncontracted. The three first *d*-type primitives are contracted using the original contraction coefficients of the $3d$ atomic orbital; all other *d*-type GTFs are not contracted.

The experimental molecular structures for the molybdenum compounds **1–6** (see Figs. 1 and 2) were taken from Refs. 44–48 and the experimental Mo chemical shifts for **1–6** were taken from Ref. 49. The experimental molecular structures and the experimental chemical shifts for tungsten compounds **7–11** (Fig. 1) are taken from a compilation of Ziegler and co-workers.[50] The molecular geometry of the thiotungstate dianion, WS_4^{2-}, was optimized using analytical gradients for the NESC-EP-B3LYP method[33] in combination with the $[16s12p8d4f]$ basis set on tungsten and the aug-cc-pVDZ basis set[43] on sulfur. An experimental geometry for WS_4^{2-} is not known and to be consistent we use the NESC-EP-B3LYP geometry rather than a geometry obtained with some other quasirelativistic approach.[50]

Calculations have been performed employing beside the B3LYP functional[38] also the BLYP (Refs. 40, 41) and the B3LYP* functionals.[51] The latter functional is a version of the standard B3LYP hybrid density functional with the amount of the HF exchange reduced from 20% to 15% as recommended by Hess *et al.*[51] In some calculations, the

Downloaded 25 Jan 2005 to 129.16.100.69. Redistribution subject to AIP license or copyright, see http://jcp.aip.org/jcp/copyright.jsp

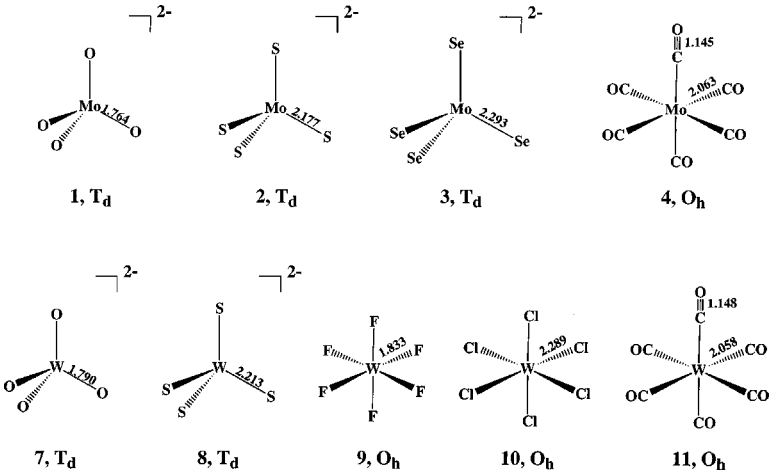

FIG. 1. Experimental geometries of molybdenum and tungsten molecules investigated in this work. Distances in Å.

functional BP86 (Ref. 52) was used to compare calculated NMR chemical shifts with results from the literature.

III. NMR CHEMICAL SHIFTS OF MOLYBDENUM AND TUNGSTEN

The isotope ^{95}Mo (spin 5/2) is measured by experimentalists because its natural abundance (15.7%) is higher than that of ^{97}Mo (spin 5/2, natural abundance 9.5%).[53] As a reference, the molybdate dianion MoO_4^{2-} in a basic solution is normally used although its shielding value is both solvent and concentration dependent (variation from 10 to −35 ppm). This of course is also true for other molybdates. For example the NMR chemical shift of ^{95}Mo in MoS_4^{2-} changes from 2176 by 78 to 2254 ppm when the solvent DMSO is replaced by water.[53]

The total NMR chemical shift range for Mo is 5500 ppm (Mo(0): −1000 to −2120 ppm; Mo(II): −2070 to −150 ppm; Mo(VI): −700 to 3350 ppm).

The only NMR-active isotope of tungsten is ^{183}W (spin 1/2), which has a natural abundance of 14.3%.[53] The tungstate dianion WO_4^{2-} is used as a reference. The chemical shift range is 9400 ppm, where the W(0) shifts are beyond −1200 ppm and W(VI) shifts are at much lower field. The chemical shifts of ^{183}W are very sensitive to the geometry and electronic structure of a tungsten compound and, therefore, can be used for structural analysis.[53] The ^{183}W shift range considered in this work is about 7000 ppm.

We calculated the ^{95}Mo and ^{183}W magnetic shieldings and NMR chemical shifts for compounds **1–11** with IGLO-DFT and IGLO-NESC-EP-DFT using the three functionals B3LYP, B3LYP*, and BLYP and the level shift operators Loc.1 and Loc.2. Results of these calculations are listed in Tables II (Mo compounds) and III (W compounds).

Common to all IGLO-B3LYP $\delta(^{95}\text{Mo})$ values is that compared to the experimental shifts they are [with the exception of the $Mo(CO)_6$ value] too positive by 200–1500 ppm. This is also found for the ^{183}W shifts, which are 80–380 ppm too positive. DFT-IGLO chemical shifts δ for first and second period nuclei are often too positive (too negative σ), which results from a DFT immanent exaggeration of the paramagnetic part leading to too positive δ.[24–27] It is noteworthy that B3LYP* and BLYP seem to produce the best NMR chemical shifts at the nonrelativistic level of theory, however the mean absolute deviations Δ are actually too large to differentiate much between the performance of the different functionals.

Apart from BLYP, relativistic corrections obtained with the IGLO-NESC-EP-DFT method lead to an improvement of both ^{95}Mo and ^{183}W shifts by reducing their absolute values (Tables II and III). By using level shift operators this im-

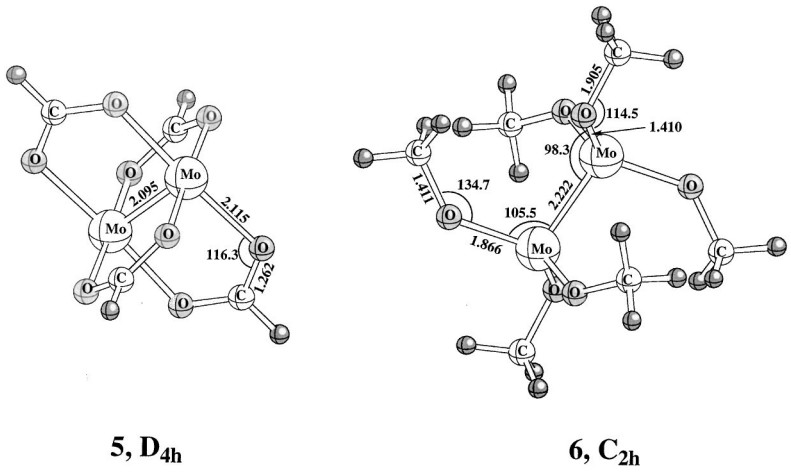

FIG. 2. Experimental geometries of molybdenum molecules with the MoMo multiple bond. Distances in Å and angles in deg.

Downloaded 25 Jan 2005 to 129.16.100.69. Redistribution subject to AIP license or copyright, see http://jcp.aip.org/jcp/copyright.jsp

TABLE II. Magnetic shieldings and NMR chemical shifts of ^{95}Mo calculated for molybdenum compounds **1–6** with different methods.[a]

Molecule	B3LYP		B3LYP*		BLYP		Expt.
	σ	δ	σ	δ	σ	δ	δ
			Nonrel.	IGLO			
MoO_4^{2-}	−1190	0	−1155	0	−1075	0	0
MoS_4^{2-}	−3687	2497	−3528	2373	−3159	2084	2259
$MoSe_4^{2-}$	−4610	3420	−4406	3251	−3874	2799	3145
$Mo(CO)_6$	1026	−2216	1072	−2227	1165	−2240	−1856
$Mo_2(O_2CH)_4$	−6433	5243	−5746	4591	−4285	3210	3702
$Mo_2(OCH_3)_6$	−4069	2879	−3739	2584	−2962	1887	2447
Δ[b]		569		323		391	
			NESC-EP	IGLO			
MoO_4^{2-}	−1017	0	−990	0	−904	0	0
MoS_4^{2-}	−3484	2467	−3352	2362	−3004	2100	2259
$MoSe_4^{2-}$	−4470	3453	−4273	3283	−3776	2872	3145
$Mo(CO)_6$	1213	−2230	1252	−2242	1327	−2231	−1856
$Mo_2(O_2CH)_4$	−5733	4716	−5141	4151	−3865	2961	3702
$Mo_2(OCH_3)_6$	−3494	2477	−3222	2232	−2579	1675	2447
Δ		387		258		464	
			Nonrel.	IGLO(Loc.1)			
MoO_4^{2-}	−1115	0	−1091	0	−996	0	0
MoS_4^{2-}	−3557	2442	−3407	2316	−3042	2046	2259
$MoSe_4^{2-}$	−4433	3318	−4236	3145	−3749	2753	3145
$Mo(CO)_6$	1067	−2182	1111	−2202	1201	−2199	−1856
$Mo_2(O_2CH)_4$	−6054	4939	−5428	4337	−4076	3080	3702
$Mo_2(OCH_3)_6$	−3939	2824	−3622	2531	−2872	1876	2447
Δ		459		224		428	
			NESC-EP	IGLO(Loc.1)			
MoO_4^{2-}	−945	0	−911	0	−832	0	0
MoS_4^{2-}	−3361	2416	−3233	2322	−2895	2063	2259
$MoSe_4^{2-}$	−4296	3351	−4092	3181	−3623	2791	3145
$Mo(CO)_6$	1250	−2195	1288	−2199	1361	−2193	−1856
$Mo_2(O_2CH)_4$	−5387	4442	−4847	3936	−3666	2834	3702
$Mo_2(OCH_3)_6$	−3382	2437	−3120	2209	−2499	1667	2447
Δ		290		183		507	
			Nonrel.	IGLO(Loc.2)			
MoO_4^{2-}	−1092	0	−1068	0	−974	0	0
MoS_4^{2-}	−3515	2423	−3366	2298	−3005	2031	2259
$MoSe_4^{2-}$	−4374	3282	−4180	3112	−3700	2726	3145
$Mo(CO)_6$	1080	−2172	1124	−2192	1213	−2187	−1856
$Mo_2(O_2CH)_4$	−5936	4844	−5328	4260	−4010	3036	3702
$Mo_2(OCH_3)_6$	−3897	2805	−3585	2517	−2843	1869	2447
Δ		423		207		444	
			NESC-EP	IGLO(Loc.2)			
MoO_4^{2-}	−923	0	−890	0	−811	0	0
MoS_4^{2-}	−3321	2398	−3194	2304	−2859	2048	2259
$MoSe_4^{2-}$	−4240	3317	−4037	3147	−3574	2763	3145
$Mo(CO)_6$	1262	−2185	1300	−2190	1372	−2183	−1856
$Mo_2(O_2CH)_4$	−5279	4356	−4754	3864	−3602	2791	3702
$Mo_2(OCH_3)_6$	−3346	2423	−3087	2197	−2473	1662	2447
Δ		264		159		523	

[a]Magnetic shieldings σ and NMR chemical shifts δ in ppm. Experimental geometries from Refs. 44–48 are used (see Figs. 1 and 2). The level shift operators Loc.1 and Loc.2 are defined in Refs. 23 and 24. Experimental NMR chemical shift values from Ref. 49.

[b]The mean absolute deviation Δ is also given in ppm.

provement can be increased. The best ^{95}Mo NMR chemical shifts are obtained with IGLO-NESC-EP-B3LYP* and the Loc.2 shift operator (mean absolute deviation Δ=159 ppm, Table II) reducing the IGLO-B3LYP* value (323 ppm, Table II) by more than 50%. A similar improvement is calculated for the ^{183}W shifts, which adopt the best agreement with experimental values at the IGLO-NESC-EP-B3LYP level of theory again with the Loc.2 shift operator (Δ=142 ppm, Table III) hardly differing from the corresponding results obtained with the B3LYP* functional (Δ=148 ppm, Table III).

Downloaded 25 Jan 2005 to 129.16.100.69. Redistribution subject to AIP license or copyright, see http://jcp.aip.org/jcp/copyright.jsp

TABLE III. Magnetic shieldings and NMR chemical shifts of ^{183}W calculated for tungsten compounds **7–11** with different methods.[a]

	B3LYP		B3LYP*		BLYP		Expt.
Molecule	σ	δ	σ	δ	σ	δ	δ
			Nonrel.	IGLO			
WO_4^{2-}	1289	0	1280	0	1223	0	0
WS_4^{2-}[b]	−2763	4052	−2675	3955	−2248	3671	3769
WF_6	2084	−795	2014	−734	1829	−606	−1121
WCl_6	−1275	2564	−1256	2536	−1196	2419	2181
$W(CO)_6$	4652	−3363	4653	−3373	4603	−3380	−3446
Δ[c]		269		250		229	
			NESC-EP	IGLO			
WO_4^{2-}	1894	0	1862	0	1784	0	0
WS_4^{2-}[b]	−2195	4089	−2145	4007	−2006	3790	3769
WF_6	2838	−944	2796	−934	2559	−775	−1121
WCl_6	−351	2245	−367	2229	−405	2189	2181
$W(CO)_6$	5565	−3671	5555	−3693	5472	−3688	−3446
Δ		197		180		154	
			Nonrel.	IGLO(Loc.1)			
WO_4^{2-}	1374	0	1346	0	1296	0	0
WS_4^{2-}[b]	−2592	3966	−2512	3858	−2293	3589	3769
WF_6	2147	−773	2074	−728	1897	−601	−1121
WCl_6	−1129	2503	−1102	2448	−1065	2361	2181
$W(CO)_6$	4687	−3313	4688	−3342	4650	−3354	−3446
Δ		250		213		243	
			NESC-EP	IGLO(Loc.1)			
WO_4^{2-}	1956	0	1926	0	1852	0	0
WS_4^{2-}[b]	−2038	3994	−1991	3917	−1858	3710	3769
WF_6	2926	−970	2832	−906	2615	−763	−1121
WCl_6	−215	2171	−231	2157	−273	2125	2181
$W(CO)_6$	5598	−3642	5590	−3664	5510	−3658	−3446
Δ		146		151		171	
			Nonrel.	IGLO(Loc.2)			
WO_4^{2-}	1400	0	1371	0	1322	0	0
WS_4^{2-}[b]	−2537	3973	−2548	3829	−2243	3565	3769
WF_6	2167	−767	2095	−724	1919	−597	−1121
WCl_6	−1080	2480	−1053	2424	−1022	2344	2181
$W(CO)_6$	4697	−3297	4698	−3327	4661	−3339	−3446
Δ		243		205		250	
			NESC-EP	IGLO(Loc.2)			
WO_4^{2-}	1977	0	1947	0	1875	0	0
WS_4^{2-}[b]	−1986	3963	−1941	3888	−1810	3685	3769
WF_6	2943	−966	2849	−902	2633	−758	−1121
WCl_6	−171	2148	−187	2134	−230	2105	2181
$W(CO)_6$	5607	−3630	5599	−3652	5520	−3645	−3446
Δ		142		148		181	

[a]Magnetic shieldings σ and NMR chemical shifts δ in ppm. Experimental geometries unless otherwise noted from Ref. 50 are used (see Fig. 1). The level shift operators Loc.1 and Loc.2 are defined in Refs. 23 and 24. Experimental NMR chemical shift values from Ref. 50.

[b]Molecular structure is optimized with the NESC-EP-B3LYP method [r(W–S)=2.213 Å].

[c]The mean absolute deviation Δ is also given in ppm.

This corresponds to an average improvement by somewhat more than 100 ppm. Clearly, the scalar relativistic corrections are important and lead at least in the case of ^{95}Mo shifts to values which are in the range of solvent corrections to the calculated shift values ±80 ppm, where the positive values can result from H-bonding and the negative values from overall electrostatic effects.

A. Analysis of relativistic corrections

For the purpose of analyzing the corrections obtained at the IGLO-NESC-EP-DFT level of theory, we have listed in Table IV diamagnetic and paramagnetic contributions to the ^{95}Mo and ^{183}W shielding values σ. Although these quantities have no relationship to measurable quantities since they are only defined within the IGLO method, they are useful for rationalizing the relativistic shift corrections.

The diamagnetic contributions are rather constant varying by just 250 ppm between 3341 and 3593 ppm in the case of ^{95}Mo shielding and 109 ppm between 7286 and 7395 ppm in the case of ^{183}W shieldings. The more a nucleus is shielded the larger becomes the corresponding diamagnetic contribution. The Mo nucleus ($Z=42$) is less shielded than

Downloaded 25 Jan 2005 to 129.16.100.69. Redistribution subject to AIP license or copyright, see http://jcp.aip.org/jcp/copyright.jsp

TABLE IV. Diamagnetic and paramagnetic contributions σ^d and σ^p to total shielding values of ^{95}Mo and ^{183}W as calculated with IGLO-NESC-EP-DFT and IGLO-DFT.[a]

	B3LYP				BLYP			
	Relativistic		Nonrelativistic		Relativistic		Nonrelativistic	
Molecule	σ^d	σ^p	σ^d	σ^p	σ^d	σ^p	σ^d	σ^p
MoO_4^{2-}	3581	−4597	3517	−4708	3584	−4488	3517	−4592
MoS_4^{2-}	3341	−6825	3277	−6964	3344	−6349	3279	−6438
$MoSe_4^{2-}$	3347	−7818	3287	−7897	3351	−7127	3289	−7163
$Mo(CO)_6$	3586	−2373	3519	−2493	3589	−2262	3522	−2357
$Mo_2(O_2CH)_4$	3593	−9325	3526	−9960	3595	−7459	3528	−7813
$Mo_2(OCH_3)_6$	3586	−7081	3519	−7589	3589	−6167	3521	−6484
WO_4^{2-}	7286	−5392	6879	−5590	7290	−5506	6883	−5661
WS_4^{2-}	7346	−9541	6934	−9697	7350	−9356	6933	−9381
WF_6	7311	−4472	6911	−4827	7316	−4757	6917	−5088
WCl_6	7373	−7724	6959	−8234	7374	−7780	6961	−8157
$W(CO)_6$	7395	−1830	7021	−2369	7397	−1925	7001	−2398

[a]Magnetic shieldings σ in ppm.

the W nucleus ($Z=74$) as reflected by the calculated diamagnetic contributions. Shielding depends also on the oxidation number of the transition metal atom and the electronegativity of the ligands attached to it. Low oxidation numbers imply larger shielding [compare, e.g., the hexacarbonyls with M(0), M=Mo, W and the compounds with M(VI) in Table IV]. In the case of compounds **5** and **6**, the oxidation states of molybdenum are II and III (the formate substituent carries one negative charge as does the alkoxy substituent) hence leading to a somewhat larger shielding in the case of **5**. An electronegative ligand can withdraw electron density and in this way lead to a deshielding of the nucleus as is the case for WF_6 relative to WCl_6. The situation is different for MoO_4^{2-}, for which the Mo nucleus is more shielded than in MoS_4^{2-} at all levels of theory (Table IV). The calculated orbital energies reveal that the nonbonding metal-centered *e*-symmetrical orbitals are more contracted (more shielding) for O than for S probably resulting from the fact that the ligand orbitals are more located at the O than at the S atoms.

The negative paramagnetic contributions vary much stronger in their magnitude (^{95}Mo by 7000 ppm; ^{183}W by 7700 ppm; Table IV) their absolute values being both larger and smaller than the diamagnetic contributions. The paramagnetic contributions are more sensitive to the electronic structure of the molecules reflecting the existence of low lying excited states (if one uses a simple sum-over-states interpretation of their values). The HOMO(t_1)-LUMO(t_1) gap decreases in the series **1**, **2**, **3** due to the fact that the splitting between the π-type bonding and antibonding ligand-metal MOs decreases with increasing electropositive character of the ligand (i.e., from O to S and Se). Similar considerations apply to the cases of compounds **9** and **10** or if one compares **1** with **7** or **2** with **8**.

Exceptionally large (negative) paramagnetic contributions are found for compounds **5** and **6**, which results from MoMo bonding in these compounds. In **5**, each Mo atom loses formally 2 electrons to the formate ligands thus changing from a Mo(0)($\cdots 4d^5 5s^1$) to a Mo(II)($\cdots 4d^4$) electron configuration, which leads to a quadruple bond. In **6**, the three methoxy ligands per Mo atom lead to a Mo(III)($\cdots 4d^3$) electron configuration and a triple MoMo bond. This is reflected in the MoMo bond lengths of 2.222 Å in the case of **6** and 2.095 Å in the case of **5** (see Fig. 2).[47,48] These values are typical for MoMo triple bond distances [measured values: 2.193–2.226 Å (Ref. 47)] and MoMo quadruple bond distances [measured values: 2.087–2.132 Å; only exception Mo_2: 1.928 Å. (Ref. 48)]. The δ*-orbital of the quadruple bond is much lower in energy than the π*-orbital of a triple bond, and the excitation energy from the bonding to the antibonding orbital is much smaller for the quadruple bond and accordingly, the paramagnetic (absolute) contribution for **5** is much larger than that for **6** (Table III).

There is a relativistic effect for both the diamagnetic and the paramagnetic contributions. For the former it is always a positive, relative constant (60–67 ppm for ^{95}Mo; 374–414 ppm for ^{183}W), and almost independent of the functional used (Table IV). Relativity leads to a contraction of the *s*- and *p*-type core orbitals thus enhancing shielding of the nucleus. This shielding effect increases with the number of core electrons. Hence, the relativistic shielding effect is almost 7 times as large for ^{183}W than for ^{95}Mo. Since the diamagnetic part concerns only the core region, for which B3LYP and BLYP provide similar descriptions, their performance does not differ.

In this connection it is interesting to note that Becke88 exchange functional[40] suffers like all gradient-corrected functionals from a singularity at the position of the nucleus. The cusp of the electron density at a nucleus leads to a singularity in the gradient of the density, which in turn results in a singularity in the exchange or correlation potential. The gradient corrections to the exchange functionals increase the absolute value of the exchange energy, the corresponding contribution to the exchange potential is therefore attractive.[40] The density cusps at the nuclei thus lead to an attractive singular contribution to the exchange potential, which increases the effective nuclear charge and the electronegativity. The strongest influence of this extra potential is to be seen for the core orbitals, which are contracted compared to LDA, leading to an increase of charge density immediately at the nucleus and a decrease in the surrounding region. This generates a shell structure in the exchange-only

Downloaded 25 Jan 2005 to 129.16.100.69. Redistribution subject to AIP license or copyright, see http://jcp.aip.org/jcp/copyright.jsp

TABLE V. Comparison of ^{183}W NMR chemical shifts calculated with the SR-HF, SO-UHF, GIAO-ZORA-DFT, and IGLO-NESC-EP-DFT method.[a]

Molecule	HF(SR)[b]	HF(SO)[b]	ZORA(SR)[c]	ZORA(SO)[c]	NESC-EP	Expt.
WO_4^{2-}	0	0	0	0	0	0
WS_4^{2-d}			3537	3638	3824	3769
WF_6	−1666	−1135	−561	−630	−761	−1121
WCl_6	1983	2685	2011	1932	2109	2181
$W(CO)_6$			−3679	−3876	−3709	−3446
Δ			299	325	188	

[a]All NMR chemical shift values in ppm. Experimental molecular geometry are used unless noted otherwise. All DFT calculations employ the BP86 density functional. Δ denotes the mean average deviation in ppm.
[b]Scalar-relativistic HF results and spin–orbit UHF results from Ref. 56.
[c]Scalar-relativistic ZORA results and ZORA results with spin–orbit coupling both taken from Ref. 50.
[d]Molecular geometry optimized by Ziegler and co-workers (Ref. 1) with the SR/BP86 method [r(W–S) = 2.231 Å] is used.

density distribution,[54] the origin of which is of mathematical rather than physical nature.

One could expect that because of the singularity in the exchange functional, screening of the nucleus and the relativistic diamagnetic correction are both exaggerated thus leading to too negative shift values. This however is not the case because the shell structure of the density close to the nucleus leads to both screening and descreening thus canceling each other largely. Hence, the too positive shift values as well as the variation in the relativistic corrections (see Tables II and III) must result from the paramagnetic contribution to the shielding values.

In the case of the paramagnetic contributions, all relativistic corrections are positive, which means that their absolute values decrease (Table IV). They vary strongly with the electronic structure of the molecule under consideration. The relativistic contraction of the *s*- and *p*-core orbitals leads also to a slight contraction of the valence *s*- and *p*-orbitals of the metal, which contribute to ligand bonding. Actually, the *d*- and *f*-type orbitals of the metal expand due to the contraction of the core orbitals and a stronger shielding of the nuclear charge. However, they are nonbonding and have no real counterparts among the unoccupied orbitals. Hence, it is the gap between the $M-L$ bonding and the $M-L$ antibonding σ and π-orbitals, which increases and leads to a reduction of the magnitude of the paramagnetic contributions. This reduction is strong in those cases, in which the (absolute) paramagnetic contribution is large (see **5** and **6**), however exceptions are also found (see, e.g., the hexacarbonyl compounds **4** and **11**). For W-compounds the relativistic corrections in the paramagnetic contributions are larger than those for the corresponding Mo-compounds due to the increase in the atomic number and the stronger relativistic contractions of the core orbitals.

Contrary to the diamagnetic contributions, the magnitude of the paramagnetic contributions depends strongly on the functional used. The improvement found for the NMR chemical shifts of ^{95}Mo and of ^{183}W when using the B3LYP* functional and when applying the level shift operator are both with regard to an improvement of the paramagnetic contributions. BLYP underestimates the magnitude of the paramagnetic contributions (values become too positive) and accordingly leads to too small shift values. If the level shift operator is applied in addition this effect is even exaggerated and leads to unreasonable NMR chemical shifts. B3LYP* in combination with relativistic corrections and the level shift operator Loc2 leads to the best calculated shift values. However, from this discussion it becomes clear that the manipulation of the exchange functional and the level shift operator fulfill the same purpose, namely, to reduce the paramagnetic contribution, which means that one correction should be able to replace the other.

B. Comparison with other theoretical results

The best values obtained in this work (IGLO/Loc2-NESC-EP-B3LYP*) are significantly better than those obtained previously with the GIAO-ZORA method for the same tungsten compounds as investigated in this work.[50] GIAO-ZORA ^{183}W NMR chemical shifts were obtained with the BP86 density functional[52] and led to a mean absolute deviation Δ of 299 ppm (Table V), which is more than 100 ppm larger than the corresponding IGLO-NESC-EP-BP86 results (Δ=188 ppm, Table V) and 150 ppm larger than the IGLO/Loc2-NESC-EP-B3LYP result (Δ=142 ppm, Table IV). Including spin–orbit (SO) coupling corrections, Δ increases even to 325 ppm (Table V).[50] Clearly, IGLO-NESC-EP-DFT offers more accurate heavy atom NMR chemical shifts than GIAO-ZORA.

The SO contribution to chemical shielding is dominated by the Fermi-contact (FC) term, which for heavy nuclei can reach values of thousands ppm. However, due to a cancellation of the FC contributions to the shielding of the reference and that of the target compound, the SO contribution to the NMR chemical shift is of the order of just 100 ppm.[55] Furthermore, the FC contribution is dominated by the shape of the potential in the vicinity of the nucleus and for a regularized potential such as in Eq. (15), the FC term differs considerably from the conventional FC term defined in the Breit–Pauli approximation (see, e.g., the discussion in Ref. 55). Consequently, the influence of the SO contribution on the IGLO-NESC-EP-DFT chemical shifts can hardly be inferred from the data obtained within different computational schemes. By analogy to ZORA chemical shift calculations[55] it can be expected that the SO contribution to ^{95}Mo and of ^{183}W NMR chemical shifts of the compounds considered in

Downloaded 25 Jan 2005 to 129.16.100.69. Redistribution subject to AIP license or copyright, see http://jcp.aip.org/jcp/copyright.jsp

this work should be comparable to solvent, concentration, and temperature effect on chemical shifts. This means that the differences between calculated and measured ^{95}Mo and of ^{183}W shifts results from SO coupling and environmental effects thus indicating that IGLO/Loc.2-NESC-EP-B3LYP* actually provides reliable shift values.

Previously, relativistically corrected NMR chemical shift calculations were carried out for a few tungsten compounds at the all-electron level with the help of finite perturbation theory employing a relativistically corrected UHF method.[56] However, in view of the relatively small $[10s9p4d1f]$ basis set used for tungsten and in view of the lack of any correlation corrections the results reported (see Table V)[56] do not compare well with the experiment and are inferior to the results obtained with DFT in the present work and by Ziegler and co-workers.[50]

IV. CONCLUSIONS

The NESC-EP approach proposed previously was combined with IGLO-DFT for calculating relativistically corrected magnetic shieldings and NMR chemical shifts. Programming and implementation of IGLO-NESC-EP-DFT leads to a computationally efficient and useful new approach for getting the magnetic properties of molecules with heavy elements.

The method was applied to calculate ^{95}Mo and ^{183}W NMR chemical shifts, which are experimentally known. The best values are obtained with IGLO-NESC-EP-DFT using the B3LYP* functional and the Loc.2 level shift operator. Mean absolute deviations of 159 ppm for ^{95}Mo and of 148 ppm for ^{183}W NMR chemical shifts are obtained. In view of the fact that the investigation included both M(0) and M(VI) oxidation states of the metal, in view of shift ranges of 5500 and 6900 ppm, respectively, in view of solvent and concentration effects of ± 80 ppm, and in view of spin–orbit corrections of ± 100 ppm results can be considered as reasonable.

Analysis of the relativistic corrections reveals that diamagnetic and paramagnetic relativistic corrections for magnetic shieldings and NMR chemical shifts differ considerably. The first is always positive, does not depend on the electronic structure of a molecule, but increases with the number of electrons of the heavy atom considered. It results from a relativistic contraction of the core *s*- and *p*-orbitals, which leads to an additional shielding of the nucleus. There is almost no dependence of the relativistic diamagnetic contributions on the exchange-correlation functional used. In the case of both the ^{95}Mo and ^{183}W chemical shifts, the relativistic corrections to the diamagnetic terms cancel largely leading to slight variations of 5 and 11 ppm, respectively, in the NMR chemical shifts, which can be neglected.

The relativistic corrections to the paramagnetic parts are also positive, i.e., the (negative) paramagnetic contributions to magnetic shieldings adopt smaller absolute values. Relativistic corrections vary in this case strongly with the electronic structure, and can be both larger and smaller than the relativistic diamagnetic corrections. With regard to the NMR chemical shifts a decrease up to 520 ppm is possible with the exception of $MoSe_4^{2-}$ for which an increase 32 ppm is found. Decreases result from the fact that the contraction of the core orbitals effects also valence *s*- and *p*-orbital thus leading to larger $\sigma(M-L)-\sigma^*(M-L)$ and $\pi(M-L)-\pi^*(M-L)$ gaps and smaller paramagnetic contributions. These effects are particularly strong when MoMo triple or quadruple bonds exist in the molecule. Similar trends are found for ^{183}W NMR chemical shifts.

The relativistic paramagnetic contributions strongly depend on the exchange correlation functional used. Differences up to 1870 ppm are found between the B3LYP and the BLYP functional where the former functional yields much better shift values than the latter functional. Best values are obtained with the B3LYP* functional, which performs at least for Mo better because it improves already the nonrelativistic shifts. Combined with relativistic corrections and level shift Loc.2 corrections it leads to the best values.

Apart from its accuracy, an important feature of the new method is its simplicity both in the sense of implementation and in the sense of computational cost. The matrix elements of the NESC-EP-DFT Hamiltonian do not involve any unusual molecular integrals often appearing in relativistic calculations; they can be evaluated analytically using the existing nonrelativistic quantum-chemical software. Since all modifications concern the one-electron Hamiltonian only, the NMR chemical shifts of a relativistic calculation can be obtained at essentially the cost of a nonrelativistic calculation.

In this work, we have not considered a spin–orbit contribution to NMR chemical shifts. This can be as large as 100 ppm as the data in Table V show. A magnetic nucleus induces a spin polarization in the nonrelativistic wave function because of the Fermi contact term thus yielding a spin–orbit contribution to the magnetic shielding already in the leading relativistic order. Since the ZORA results[50] differ considerably from the NESC-EP-DFT results of this work, it makes little sense to speculate about additional spin–orbit corrections. Work is in progress to obtain genuine spin–orbit corrections within the NESC-EP-DFT method.

ACKNOWLEDGMENTS

This work was supported by the Swedish Research Council (Vetenskapsrådet). An allotment of computer time at the National Supercomputer Center (NSC) at Linköping is gratefully acknowledged.

[1] See, e.g., *Encyclopedia of Nuclear Magnetic Resonance*, edited by D. M. Grant and R. K. Harris (Wiley, Chichester, 1996), Vols. 1–8, and articles therein.
[2] T. Helgaker, M. Jaszuński, and K. Ruud, Chem. Rev. **99**, 293 (1999).
[3] D. Cremer, L. Olsson, F. Reichel, and E. Kraka, Isr. J. Chem. **33**, 369 (1993).
[4] J. Gauss, Ber. Bunsenges. Phys. Chem. **99**, 1001 (1995).
[5] T. D. Bouman and A. E. Hansen, Chem. Phys. Lett. **175**, 292 (1990).
[6] (a) J. Oddershede and J. Geertsen, J. Chem. Phys. **92**, 6036 (1990); (b) S. P. A. Sauer, I. Paidarova, and J. Oddershede, Mol. Phys. **81**, 87 (1994); (c) Theor. Chim. Acta **88**, 351 (1994).
[7] (a) J. Gauss, Chem. Phys. Lett. **191**, 614 (1992); (b) J. Chem. Phys. **99**, 3629 (1993).
[8] J. Gauss, Chem. Phys. Lett. **229**, 198 (1994).
[9] (a) J. Gauss and J. F. Stanton, J. Chem. Phys. **102**, 251 (1995); (b) **103**, 3561 (1995).
[10] J. Gauss and J. F. Stanton, J. Chem. Phys. **104**, 2574 (1996).

Downloaded 25 Jan 2005 to 129.16.100.69. Redistribution subject to AIP license or copyright, see http://jcp.aip.org/jcp/copyright.jsp

[11] J. Gauss and J. F. Stanton, Adv. Chem. Phys. **123**, 355 (2002).
[12] K. Ruud, T. Helgacker, R. Kobayashi, P. Jørgensen, K. L. Bak, and H. J. Aa. Jensen, J. Chem. Phys. **100**, 8178 (1994).
[13] C. van Wüllen and W. Kutzelnigg, Chem. Phys. Lett. **205**, 563 (1993).
[14] A. E. Hansen and T. D. Bouman, J. Chem. Phys. **82**, 5035 (1985).
[15] J. Oddershede, P. Jørgensen, and D. L. Yeager, Comput. Phys. Rep. **2**, 33 (1984).
[16] (a) F. London, J. Phys. Radium **8**, 397 (1937); (b) H. Hameka, Mol. Phys. **1**, 203 (1958); (c) R. Ditchfield, *ibid.* **27**, 789 (1974).
[17] K. Wolinski, J. H. Hinton, and P. Pulay, J. Am. Chem. Soc. **112**, 8251 (1990).
[18] M. Häser, R. Ahlrichs, H. P. Baron, P. Weis, and H. Horn, Theor. Chim. Acta **83**, 455 (1992).
[19] (a) G. Rauhut, S. Puyear, K. Wolinski, and P. Pulay, J. Phys. Chem. **100**, 6310 (1996); (b) J. R. Cheeseman, G. W. Trucks, T. A. Keith, and M. J. Frisch, J. Chem. Phys. **104**, 5497 (1996).
[20] (a) G. Schreckenbach and T. Ziegler, Int. J. Quantum Chem. **61**, 899 (1997); (b) S. K. Wolff and T. Ziegler, J. Chem. Phys. **109**, 895 (1998); (c) R. Bouten, E. J. Baerends, E. van Lenthe, L. Visscher, G. Schreckenbach, and T. Ziegler, J. Phys. Chem. A **104**, 5600 (2000).
[21] (a) W. Kutzelnigg, Isr. J. Chem. **19**, 193 (1980); (b) M. Schindler and W. Kutzelnigg, J. Chem. Phys. **76**, 1919 (1982).
[22] W. Kutzelnigg, U. Fleischer, and M. Schindler, in *NMR, Basic Principle and Progress*, edited by P. Diehl, E. Fluck, H. Günther, R. Kosfeld, and J. Seelig (Springer, Berlin, 1990), Vol. 23, p. 165.
[23] V. G. Malkin, O. L. Malkina, M. E. Casida, and D. R. Salahub, J. Am. Chem. Soc. **116**, 5898 (1994).
[24] L. Olsson and D. Cremer, J. Chem. Phys. **105**, 8995 (1996).
[25] L. Olsson and D. Cremer, J. Phys. Chem. **100**, 16881 (1996).
[26] (a) E. Kraka, C. P. Sosa, and D. Cremer, Chem. Phys. Lett. **260**, 43 (1996); (b) K. Schroeder, W. Sander, R. Boese, S. Muthusamy, A. Kirschfeld, E. Kraka, C. Sosa, and D. Cremer, J. Am. Chem. Soc. **119**, 7265 (1997); (c) L. Olsson and D. Cremer, Chem. Phys. Lett. **215**, 413 (1993); (d) C.-H. Ottosson and D. Cremer, Organometallics **15**, 5495 (1996).
[27] C.-H. Ottosson, E. Kraka, and D. Cremer, in *Theoretical and Computational Chemistry, Pauling's Legacy: Modern Modeling of the Chemical Bonding*, edited by Z. B. Maksić (Elsevier, Amsterdam, 1999), Vol. 6, p. 231.
[28] M. Kollwitz and J. Gauss, Chem. Phys. Lett. **260**, 639 (1996).
[29] A. M. Lee, N. C. Handy, and S. M. Coldwell, J. Chem. Phys. **103**, 10095 (1995).
[30] (a) V. Polo, E. Kraka, and D. Cremer, Mol. Phys. **100**, 1771 (2002); (b) V. Polo, E. Kraka, and D. Cremer, Theor. Chem. Acc. **107**, 291 (2002); (c) V. Polo, J. Gräfenstein, E. Kraka, and D. Cremer, Chem. Phys. Lett. **352**, 469 (2002); (d) V. Polo, J. Gräfenstein, E. Kraka, and D. Cremer, Theor. Chem. Acc. **109**, 22 (2003).
[31] D. Cremer, Mol. Phys. **99**, 1899 (2001).
[32] M. Filatov and D. Cremer, Theor. Chem. Acc. **108**, 168 (2002).
[33] M. Filatov and D. Cremer, Chem. Phys. Lett. **351**, 259 (2002).
[34] M. Filatov and D. Cremer, Chem. Phys. Lett. **370**, 647 (2003).
[35] (a) K. G. Dyall, J. Chem. Phys. **106**, 9618 (1997); (b) **109**, 4201 (1998).
[36] W. Kohn and L. J. Sham, Phys. Rev. **140**, 1133 (1965).
[37] S. F. Boys, in *Quantum Theory of Atoms, Molecules, and Solid State*, edited by P. O. Löwdin (Interscience, New York, 1967), p. 253; J. M. Foster and S. F. Boys, Rev. Mod. Phys. **32**, 296 (1960).
[38] (a) A. D. Becke, J. Chem. Phys. **98**, 5648 (1993); (b) P. J. Stephens, F. J. Devlin, C. F. Chabalowski, and M. J. Frish, J. Phys. Chem. **98**, 11623 (1994).
[39] E. Kraka, J. Gräfenstein, J. Gauss *et al.*, COLOGNE 2003 (Göteborg University, Göteborg, 2003).
[40] A. D. Becke, Phys. Rev. A **38**, 3098 (1988).
[41] C. Lee, W. Yang, and R. G. Parr, Phys. Rev. B **37**, 785 (1988).
[42] O. Gropen, J. Comput. Chem. **8**, 982 (1987).
[43] T. H. Dunning, Jr., J. Chem. Phys. **90**, 1007 (1989).
[44] T. J. R. Weakley, Acta Crystallogr., Sect. C: Cryst. Struct. Commun. **43**, 2221 (1987).
[45] M. G. Kanatzidis and D. Coucouvanis, Acta Crystallogr., Sect. C: Cryst. Struct. Commun. **39**, 835 (1983).
[46] S. C. O'Neal and J. W. C. Olis, J. Am. Chem. Soc. **110**, 1971 (1988).
[47] (a) G. A. Robbins and D. S. Martin, Inorg. Chem. **23**, 2086 (1984). For other typical MoMo quadruple bond distances, see (b) F. A. Cotton, E. V. Dikarev, and S. Herrero, *ibid.* **38**, 2649 (1999); (c) S. Roszak and K. Balasubramanian, *ibid.* **33**, 4169 (1994).
[48] (a) M. H. Chisholm, F. A. Cotton, C. A. Murillo, and W. W. Reichert, Inorg. Chem. **16**, 1801 (1977). For other typical MoMo triple bond distances, see (b) M. H. Chisholm, K. Folting, W. E. Streib, and D. D. Wu, *ibid.* **38**, 5219 (1999).
[49] P. S. Pregosin, in *Transition Metal Nuclear Magnetic Resonance*, edited by P. S. Pregosin (Elsevier, Amsterdam, 1991), pp. 67–81.
[50] A. Rodriguez-Fortea, P. Alemany, and T. Ziegler, J. Phys. Chem. A **103**, 8288 (1999).
[51] M. Reiher, O. Salomon, and B. A. Hess, Theor. Chem. Acc. **107**, 48 (2001).
[52] (a) A. Becke, Phys. Rev. A **38**, 3098 (1988); (b) J. Perdew, Phys. Rev. B **33**, 8822 (1986).
[53] (a) P. Granger, in *NMR of Newly Accessible Nuclei. Chemical and Biochemical Applications*, edited by P. Laszlo (Academic, New York, 1983), Vol. 1, p. 385. For tungsten NMR chemical shifts, see also (b) B. E. Mann, in *Annual Reports on NMR Spectroscopy*, edited by G. A. Webb (Academic, New York, 1994).
[54] Y. He, J. Gräfenstein, E. Kraka, and D. Cremer, Mol. Phys. **98**, 1639 (2000).
[55] S. K. Wolff, T. Ziegler, E. van Lenthe, and E. J. Baerends, J. Chem. Phys. **110**, 7689 (1999).
[56] M. Hada, H. Kaneko, and H. Nakatsuji, Chem. Phys. Lett. **261**, 7 (1996).

Downloaded 25 Jan 2005 to 129.16.100.69. Redistribution subject to AIP license or copyright, see http://jcp.aip.org/jcp/copyright.jsp